

# Silver Surfaces with Optimized Surface Enhancement by Self-Assembly of Silver Nanoparticles for Spectroelectrochemical Applications

Marc Grosserueschkamp,<sup>†,‡</sup> Christoph Nowak,<sup>†,‡</sup> Denise Schach,<sup>†,‡</sup> Wolfgang Schaertl,<sup>§</sup> Wolfgang Knoll,<sup>‡</sup> and Renate L. C. Naumann<sup>\*,†</sup>

Max Planck Institute for Polymer Research, Ackermannweg 10, 55128 Mainz, Germany; Austrian Research Centers GmbH, Tech Gate Vienna, Donau-City Str. 1, 1220 Vienna, Austria; and Johannes Gutenberg-Universität Mainz, Saarstrasse 21, 55099 Mainz, Germany

Received: June 15, 2009; Revised Manuscript Received: August 21, 2009

A surface was developed for surface-enhanced resonance Raman spectroscopy in the near-ultraviolet range. For this purpose, silver nanoparticles were synthesized, exhibiting localized surface plasmon resonance at an excitation wavelength of 410 nm. The nanoparticles were adsorbed onto the plane of a silver rod where the number of particles per unit area was controlled by the adsorption time. SERR spectra of cytochrome *c* were used as a reference system to quantify the enhancement factor of the newly developed surface. Optimal enhancement was obtained when the individual nanoparticle coverage on the surface reached a maximum. Nanoparticles touching each other in pairs or clusters led to shifts in the resonance frequency of resonantly coupled localized surface plasmons. Clusters therefore did not contribute to the enhancement factor at the wavelength of 413 nm. The overall surface enhancement factor finally achieved at this particular wavelength was in the range of  $10^4$ – $10^5$ .

## Introduction

Raman scattering is a weak photon–molecule interaction. The Raman scattering cross section is on the order of magnitude of  $10^{-30}$  cm<sup>2</sup>.<sup>1</sup> Nevertheless, Raman spectroscopy has become an important analytical tool in many fields of science, such as chemistry, medicine, and the life sciences.<sup>2–5</sup> This is mainly due to the fact this technique experienced a dramatic impulse by the discovery of the surface enhancement effect of roughened surfaces by Fleischmann et al.<sup>6</sup>

Different mechanisms contribute to the enhanced Raman scattering of molecules adsorbed on rough metal substrates. The electromagnetic enhancement effect<sup>7</sup> (EMEE) and the chemical enhancement effect (CEE),<sup>8</sup> the latter also known as charge transfer effect, are of great interest in this context. The EMEE is based on collective electron oscillations in resonance with the exciting laser wavelength yielding high electromagnetic field enhancement in the proximity of the metal surface.<sup>9</sup> In the literature such electron oscillations are often referred to as localized surface plasmons (LSP), particularly if they are excited within nanoscopic metal structures such as colloids or rough surface bumps. When two or more nanostructures approach each other to an extent where there is an overlap between the electromagnetic (EM) fields radiated by the LSPs, so-called coupled LSP oscillations may occur.<sup>10–13</sup> Coupled LSP exhibit an even higher EM field enhancement in the gap between two nanoparticles (NP).<sup>14</sup> These gaps between resonantly coupled NPs are referred to as “hot spots”. Moreover, the resonance frequency of such complexes can be shifted away from the frequency of single NPs.<sup>15</sup> Touching particle pairs exhibit a conductive bridge in the plane of electron oscillation and are thus capable of being excited with additional LSP modes at

lower frequencies.<sup>12,15</sup> At the same time the primary modes are still red-shifted as in the case of nearly touching particles.<sup>13,15</sup> The EMEE is capable of enhancing the intensity of Raman spectra of all molecules in close proximity to the metal substrate. Contrary to the EMEE, the CEE only occurs if the probed molecules are adsorbed on the surface. The underlying mechanism is a charge-transfer resonance between the metal substrate and the adsorbed molecule. Assuming the Fermi level of the metal is located between the ground state and an excited state of the molecule, charge transfer transitions from the Fermi level to the excited state, as well as transitions from the ground state to the Fermi level, can contribute to the CEE.<sup>16,17</sup>

Although these effects are now well understood, it is still difficult to differentiate between contributions from EMEE and CEE. EM enhancement may be observed in the absence of chemical enhancement when the molecules are not adsorbed to the metal substrate. In contrast, chemical enhancement is always accompanied by EM enhancement. Notwithstanding the enhancement effects, poor signal-to-noise ratios in Raman spectra are an inherent problem of the weak scattering process. Particularly low intensities are observed while probing a monolayer of molecules in the case of spectroelectrochemistry. The short accumulation time of time-resolved spectra further limits the quality of the spectra. Nevertheless, spectroelectrochemistry as well as time-resolved Raman spectroscopy in combination with the surface enhancement gives access to parameters such as rate constants of electron transfer or conformational changes in proteins inaccessible by normal Raman experiments.<sup>18</sup> In the majority of surface-enhanced (resonance) Raman scattering (SER(R)S) experiments, however, electrochemically roughened silver electrodes were employed.<sup>18–20</sup> A drawback of this technique is that the enhancement effect is hard to control. It heavily depends on the exact conditions of the oxidation–reduction cycle (ORC), i.e., the duration and magnitude of the applied potential as well as the molarity of the salt solution. Nevertheless, Taylor et al.<sup>21</sup> reported a typical

\* Corresponding author: Tel +49 6131 379 157, Fax +49 6131 379 100, e-mail naumannr@mpip-mainz.mpg.de.

<sup>†</sup> Max Planck Institute for Polymer Research.

<sup>‡</sup> Austrian Research Centers GmbH.

<sup>§</sup> Johannes Gutenberg-Universität Mainz.

enhancement factor of  $2 \times 10^4$  for such substrates. Wen and Fang<sup>22</sup> made an attempt to improve the enhancement factor by adsorbing silver nanoparticles on electrochemically roughened silver electrodes. This technique, however, was not designed to overcome the high surface roughness obtained by any kind of ORC. The high roughness does not allow the arrangement of well-ordered monolayers, often significant in the context of electrochemical processes. Moreover, controlling the enhancement effect remains a problem due to irregularities of the underlayer.

In order to overcome these drawbacks, we made an attempt to develop a SERR-active surface by the adsorption of silver colloids on a planar silver surface. Varying the amount of adsorbed NPs gave us the advantage of a controlled enhancement effect. Moreover, the roughness was dramatically reduced compared to the electrochemical roughening as it was determined only by the size of the colloids. Such LSP of nanostuctures have been reported before, however, on dielectric or semiconductive surfaces such as glass, silicon, or ITO.<sup>12,13,23</sup> Colloidal particles are not conductively connected in this case, unlike the conducting silver surface. Possible effects of this conductive connection were investigated together with the effect of the distribution of NPs on the Ag surface. The number of NPs on the surface was controlled by varying the adsorption time. The correlation between the number of NPs and Raman intensity was examined using, as a reference, cytochrome *c* (cc) adsorbed to a monolayer of mercaptoethanol. LSP resonance was excited with the 413 nm line of a Kr<sup>+</sup> laser.

## Materials and Methods

**1. Fabrication of Silver Nanoparticles.** Silver nanoparticles (AgNPs) were synthesized according to a modified version of the method of Turkevich<sup>24</sup> and Frens,<sup>25</sup> who introduced citric acid as a reducing agent. 8.25 mL of 37% formaldehyde was added to 250 mL of an aqueous AgNO<sub>3</sub> solution (10 mM/L). The mixture was heated during vigorous stirring to 100 °C for at least 15 min. Then 4 mL of an aqueous solution of citric acid (33 mM/L) was added. The temperature was kept constant at 100 °C until the color changed in the first minutes to a bright yellow, eventually changing into a darker greenish-yellow, indicating a suspension of AgNPs.

**2. Dynamic Light Scattering (DLS).** DLS was performed with a setup from ALV (ALV-Laser Vertriebsgesellschaft mbH, Langen, Germany). It consists of a HeNe laser as the light source, a goniometer (ALV-Laser Vertriebsgesellschaft mbH, Langen, Germany) to control the detector angle, and a fiber-optic detector to measure the intensity of the scattered light. The width of the laser beam was reduced to 1 mm by using a two-lens system. The size distribution of the AgNPs was obtained from intensity time correlation functions obtained from the homodyne detected scattered intensity using an ALV 5000 hardware correlator. The AgNP suspension obtained from the procedure described above was diluted at a ratio of 1:10. Dust particles were removed from the suspension by filtration with Millipore filters; pore size 0.45 μm. Cylindrical Suprasil light scattering cuvettes of 10 mm diameter were used. The cuvettes were kept in a temperature-controlled toluene bath to avoid diffraction from the glass walls.

**3. Surface Modification.** The top planes of 12 mm thick silver rods were polished as described before<sup>18</sup> down to a rms roughness of 3–5 nm. Self-assembled monolayers (SAMs) were formed by immersion of the silver rods into an aqueous solution of cysteamine (CA) (10 mM/L) for 1 h. After thorough rinsing with water the modified silver rods were immersed into the

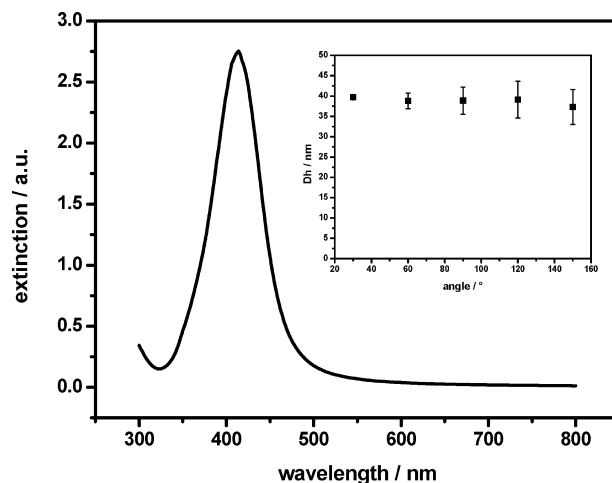


**Figure 1.** UV-vis spectrum of AgNPs in solution. A distinct local maximum at 410 nm indicates the LSP resonance of the nanospheres. Inset: DLS data. The average size of the AgNPs amounts to 39 nm.

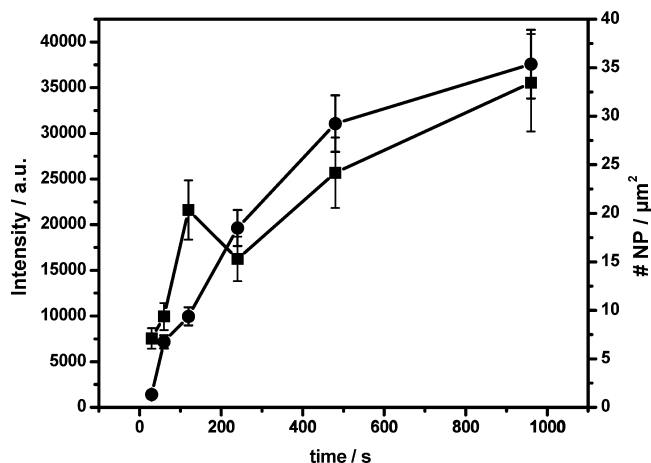


**Figure 2.** Raman intensity of the  $\nu_4$  band plotted as a function of NP adsorption time (squares) compared to the total number of NPs adsorbed on the surface (circles). The Raman intensity is proportional to the number of NPs as long as the interparticle distance does not allow for LSP coupling of neighboring NPs.

nanoparticle suspension for different periods of time indicated below. The silver rods were then rinsed with water again before immersing them into a solution of mercaptoethanol (ME) (10 mM/L) for at least 1 h to form a SAM of ME, thus displacing residual CA molecules from the surface. Finally, after rinsing with water, cc was adsorbed on the functionalized silver electrode from a solution of cc (50 μM/L) in PBS buffer (20 mM/L K<sub>2</sub>HPO<sub>4</sub>/100 mM/L NaClO<sub>4</sub>/pH = 7) for at least 30 min.

**4. Raman Experiments.** The setup used for Raman experiments was described in detail in a previous publication.<sup>18</sup> All Raman experiments were performed using the 413 nm line of a Kr<sup>+</sup> laser (Innova 90C, Coherent). After passing a premonochromator (LaserspecIII, Spectrolab Research Laboratory, Newbury, England) the laser beam was coupled into a confocal Raman microscope (LabRam, HR800, HORIBA Jobin Yvon) equipped with a water immersion objective (Olympus LUMPLFL, 100 XW, WD = 1.5, NA = 1, BFOBJ). By this means the laser beam was focused on top of the modified plane of the silver rod immersed in PBS. The scattered light was filtered by a holographic notch filter and guided to an 1800 grooves/mm grating providing spectral resolution. The spectrum was imaged onto a liquid nitrogen cooled back-illuminated CCD detector (Symphony, Jobin Yvon).

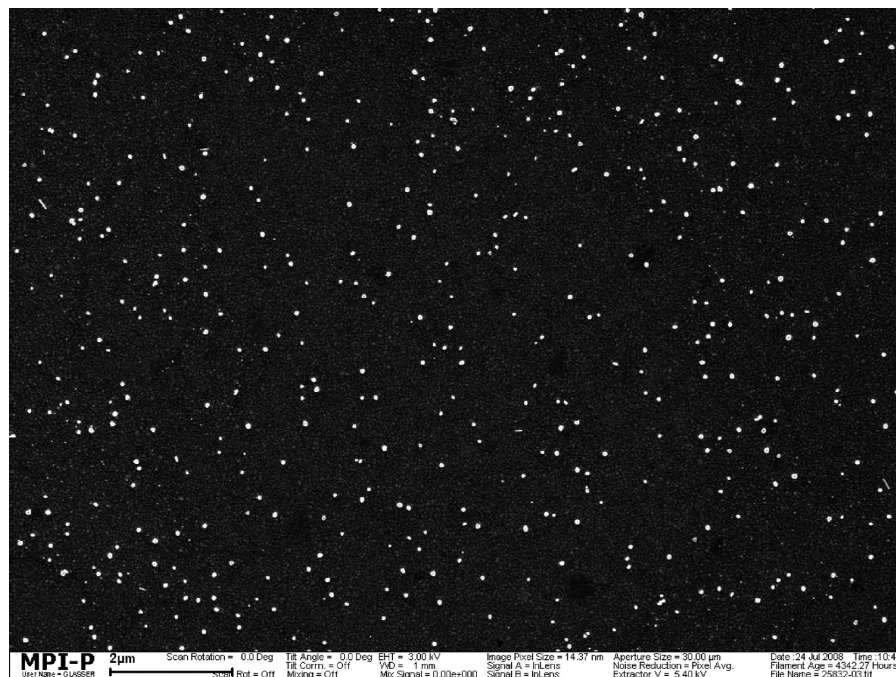


**Figure 3.** REM image of AgNPs after an adsorption time of 16 min. Individual NPs are strictly separated from each other; hence, no particle interactions occur.

**5. Scanning Electron Microscopy (SEM).** SEM images of the same samples that had been used for the Raman measurements were taken using a SEM instrument (1530 Gemini, Leo/Carl Zeiss SMT - Nano Technology Systems). Images were recorded showing exaggerated contrast in order to allow for automated particle counting.

## Results and Discussion

Silver nanoparticles were fabricated by the method developed by Turkevich and Frens using citric acid as a reducing agent. The additional use of formaldehyde proved very effective in suppressing cluster formation. As a result, dynamic light scattering (DLS) revealed a highly monodisperse solution of spherical NPs of an average size of 39 nm (inset, Figure 1). UV-vis spectra of the colloidal suspension showed a distinct maximum of the extinction at a wavelength of 410 nm. This corresponds to the wavelength of the laser beam (413 nm) used for the excitation of the Raman scattering. The absorbance maximum of 410 nm indicates the excitation of localized surface plasmons within the NPs at this particular wavelength (Figure 1).

AgNPs thus formed are characterized by a negatively charged envelope of citric acid, which enables them to adsorb on the positively charged monolayer of cysteamine (CA) on the flat surface of a silver rod. Once adsorbed, the NPs could not be removed by rinsing with water or other solutions, even those containing thiols such as mercaptoethanol (ME). Such a solution was later used to modify the outer surface of the assembly of AgNPs with yet another monolayer of ME. Particles were assembled on the surface by immersion into the suspension of AgNPs at the concentration as obtained by the preparation procedure described above.

The number of AgNPs per unit area adsorbed on the SAM of CA was controlled by varying the time of immersion of the polished silver rods in the colloidal suspension. The number of particles finally obtained was taken from REM images of the

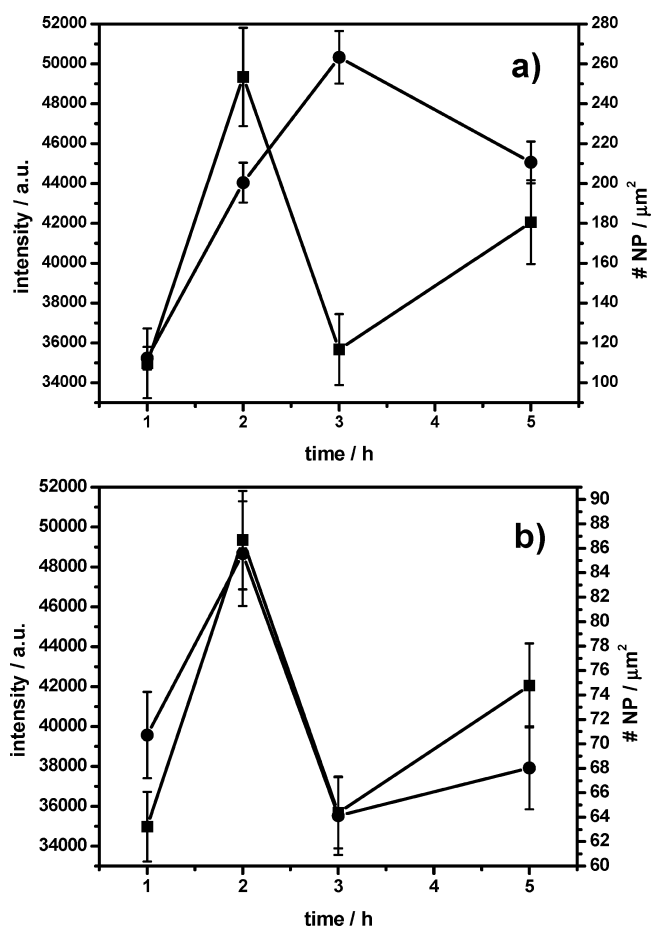


**Figure 4.** Raman intensity of the  $\nu_4$  band plotted as a function of NP adsorption time (squares) compared to (a) the total number of NPs adsorbed on the surface (circles) and (b) the number of strictly separated NPs. The Raman intensities do not correlate with the total number of NPs, but instead with the number of strictly separated NPs.



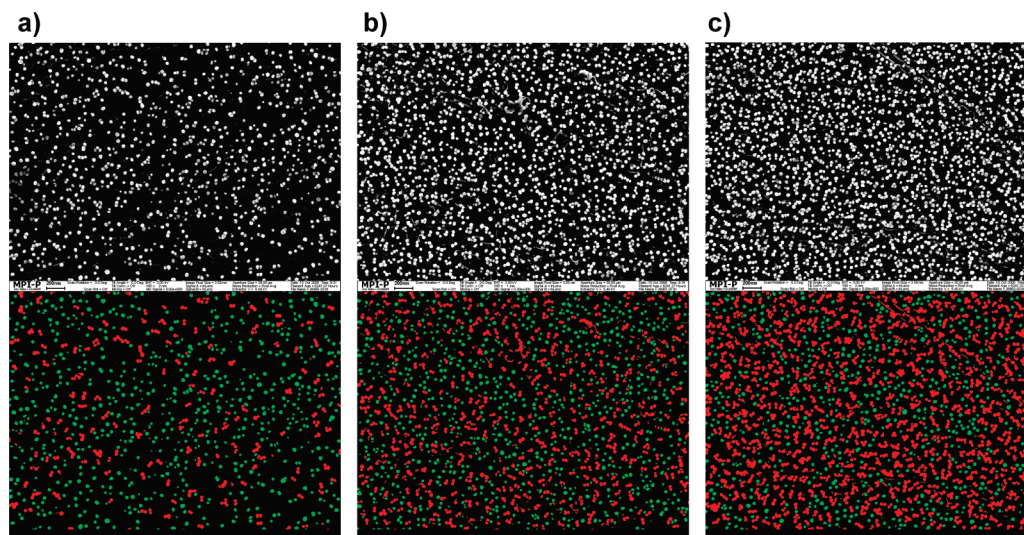


**Figure 5.** REM images of NPs after adsorption times of 1 (a), 2 (b), and 3 (c) h. The total amount of NPs increases from 1 to 3 h adsorption time. The lower row shows the same REM images with particle clusters and separated particles colored red and green, respectively. The amount of particle clusters increases from 1 to 3 h adsorption time, while the amount of separated NPs reaches its maximum after 2 h.

modified surfaces. Particle counting was done by the software ImageJ. Within a range of minutes ( $\leq 16$  min) the number of particles increased up to  $35 \text{ NPs}/\mu\text{m}^2$  as a function of the immersion time (Figure 2). For each data point 2–3 different samples have been analyzed at 2–3 different spots. The error bars given in the figures represent the experimental error (e.g., particle counting) as well as the sample-to-sample deviation. Particles were explicitly separated from each other in this regime (Figure 3). This was not the case when immersion times were longer than 16 min. At a certain particle density ( $\sim 100 \text{ NPs}/\mu\text{m}^2$  or after 1 h) adsorption of further particles no longer correlated with time anymore. After 3 h, the particle density reached  $\sim 270 \text{ NPs}/\mu\text{m}^2$ , and a further adsorption of NPs could not be observed (Figure 4). This might be due to repulsive forces originating from the surface charges of the silver spheres. The highest enhancement was not observed on surfaces with the highest NP coverage. Hence, not all NPs contribute to the EM field enhancement as in the low particle density regime. The highest enhancement was achieved after an adsorption time of  $\sim 2$  h when a particle density of  $\sim 200 \text{ NPs}/\mu\text{m}^2$  was reached. Further adsorption of NPs did not lead to higher peak intensities, but to a decrease in enhancement. In fact, a definite correlation between the total amount of NPs and the peak intensities in the Raman spectra was not found (Figure 4a).

This behavior was correlated with the enhancement effect by measurements of SERR spectra of cc adsorbed on the different surfaces via a monolayer of ME. For this purpose the Raman band  $\nu_4$  at  $1374 \text{ cm}^{-1}$  of oxidized cc resulting from a distortion mode of the pyrrole half-ring<sup>26</sup> was used as a marker band. Its peak intensity was then correlated with the surface enhancement. In the low particle density regime ( $< 16$  min) the peak intensity of the  $\nu_4$  band was directly proportional to the number of particles. Hence, all the NPs contributed equally to the observed signal by enhancing the EM field in close proximity of the individual particles (Figure 2).

In order to investigate this behavior more closely, we conducted a detailed analysis of the particle distribution using the software ImageJ (particle detection and counting) and Gimp2.0 (image processing), from REM images (Figure 5). This allowed us to discriminate between separate NPs (green) and clusters of adhering NPs (red). The distribution across the plane of the silver surface revealed a steady increase of clusters of

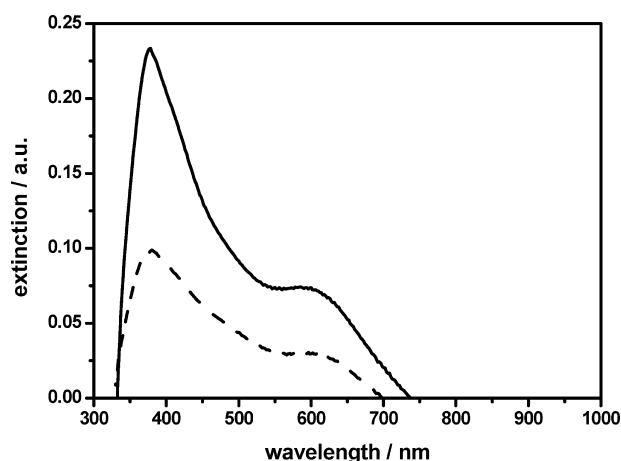


**Figure 6.** Spectrum of NPs adsorbed on a 50 nm Ag film on a glass substrate after adsorption times of 1 h (lower trace) and 2 h (upper trace). Local maxima of the extinction are observed at around 390 and 600 nm due to LSP resonance of separated NPs and particle clusters, respectively.

particles in direct contact and therefore forming conductive bridges between neighboring particles (Figure 5). A strict discrimination between separated NPs and those arranged in clusters gives evidence of the correlation between the peak intensities of Raman spectra and the amount of separate NPs (Figure 4b). NPs arranged in clusters of two or more particles did not contribute to the enhanced Raman signal. UV–vis spectroscopy revealed large shifts to higher wavelengths in the LSP resonance of particle aggregates (Figure 6). The spectra were recorded using 50 nm evaporated silver on a glass slide as a substrate for AgNP adsorption. The two local extinction maxima at 390 and 600 nm resulted from different modes of LSP resonance. They were assigned to the LSP resonance of separated NPs and the particle clusters of two or more particles, respectively. Thus, NP aggregates were not amenable to the excitation of LSPs at the same wavelength as a single NP. Consequently, they did not contribute to surface-enhanced Raman scattering. Large red shifts in the resonance frequency of particles touching each others were shown previously, both theoretically and experimentally.<sup>12,13,23</sup>

Nevertheless, the resonance frequency of the LSP of single NPs was still in a range to be excited with the 413 nm laser

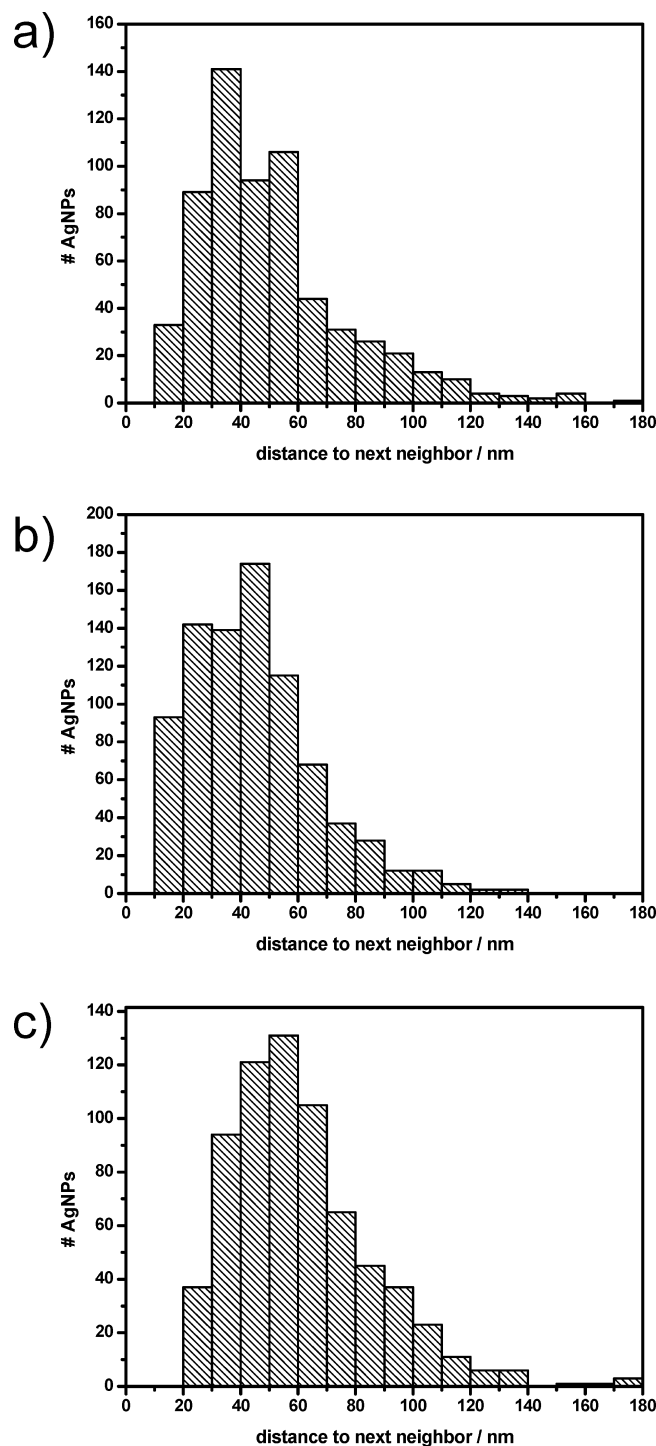


**Figure 7.** Histograms show the statistical distribution of the distance to the next neighbor for each particle. The NP adsorption times were 1 (a), 2 (b), and 3 h (c). The average distances to the next neighbor were 51, 45, and 51 nm, respectively.

line, although Ag was used as a conductive substrate in contrast to the work of others, who used dielectric substrates such as glass. However, the extinction maximum of isolated AgNPs was slightly downshifted to  $\sim 390$  nm. This effect can be explained in terms of the permittivity of the surrounding media of the AgNPs, which is known to affect the LSP resonance frequency. In the case of the AgNP suspension the surrounding medium was basically water, while in the case of adsorbed NPs, the NPs were surrounded by air. The permittivity of water exceeds the permittivity of air, whereby LSP resonance is shifted to higher energies.

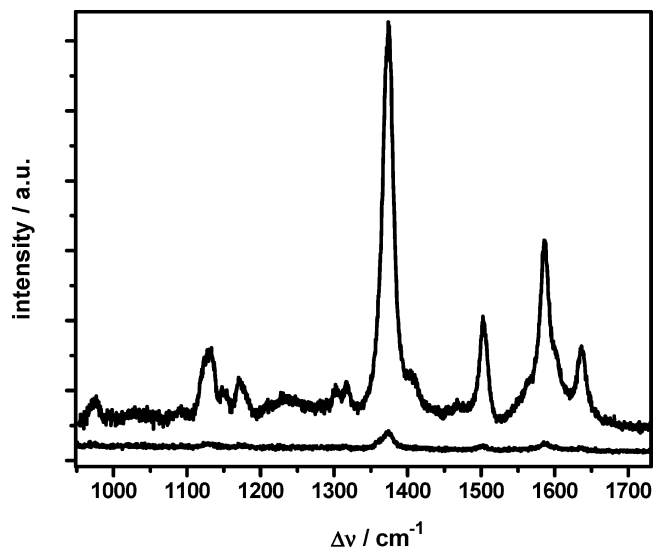


**Figure 8.** Raman spectra of cytochrome *c* adsorbed on a layer of AgNPs (upper trace) and adsorbed on the plane of a polished silver electrode (lower trace).

A conductive substrate was employed in order to perform spectroelectrochemical measurements. Therefore, all NPs were in electric contact with each other via the plane of the silver electrode. This did not seem to affect the resonance frequency of the LSP. We concluded that optical properties of NP assemblies are affected only by conductive bridges in the plane of local electron oscillations.

As a further parameter of the image analysis, the average distance to the next neighbor (NN) was obtained (Figure 7). Single, nontouching NPs were separated by 45–51 nm on average, the distance being in the range of the particle diameter. In the case of 2 h assembly time, the distribution of NN shows a tendency to distance lower than the NP diameter, as compared to both the 1 and 3 h. This could explain the slightly disproportional increase in Raman intensity compared to the increase in separated NPs after an adsorption time of 2 h. The effect might be due to such coupled LSPs and the increase in the EM field strength as a consequence of the coupling effect. However, from the distance distribution to the NN we concluded that coupled LSP are of importance for only a minor fraction of the separated NPs.

In Figure 8, the Raman scattering spectra of *cc* is depicted. The AgNP-modified substrate used in this case was prepared under the conditions found to be optimal in terms of Raman signal enhancement; i.e., AgNPs were allowed to adsorb for 2 h. The signal accumulation time was 15 s, and the laser power was adjusted to less than  $100 \mu\text{W}$ . A REM image of this AgNP substrate is shown in Figure 9. Finally, the total average SERS enhancement factor was calculated according to<sup>27</sup>

$$\text{EF} = \frac{I_{\text{SERRS}} N_{\text{surf}}}{I_{\text{RR}} N_{\text{vol}}} \quad (1)$$

with  $I_{\text{SERRS}}$  and  $I_{\text{RR}}$  the Raman intensity observed on the SERRS-active surface and in solution, respectively, and  $N_{\text{surf}}$  and  $N_{\text{vol}}$  the number of sampled molecules adsorbed on the surface and in solution.  $N_{\text{surf}}$  and  $N_{\text{vol}}$  was estimated respectively to be  $3.75 \times 10^6$  and  $3.75 \times 10^8$  molecules from the peak area of cyclic voltammograms of cytochrome *c* (data not shown) and the molarity of the sample solution and the volume illuminated by the laser. The SERRS intensity was  $\sim 100$  times higher compared to the resonance Raman intensity, while the signal

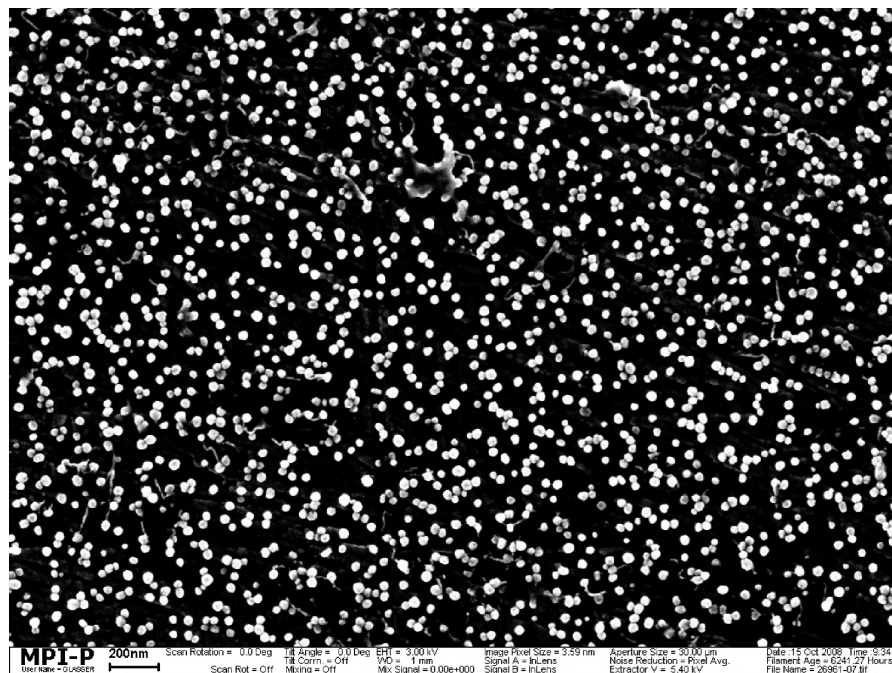


**Figure 9.** REM images of AgNPs after an adsorption time of 2 h. The image illustrates the narrow distribution in size of the adsorbed NPs. Most NPs are separated from their next neighbor, but a small fraction is arranged in clusters of two or more particles.

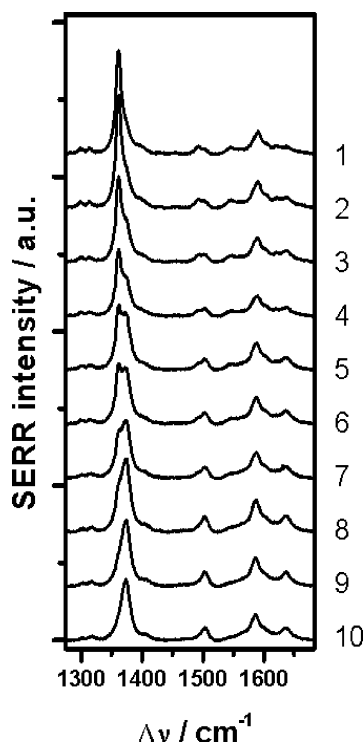


**Figure 10.** Potentiostatic titration of cc by SERRS. Spectra of cc were acquired at different static potentials applied to the protein immobilized on the SERR-active Ag surface. (1)  $-50$ , (2)  $+20$ , (3)  $+80$ , (4)  $+130$ , (5)  $+170$ , (6)  $+190$ , (7)  $+210$ , (8)  $+250$ , (9)  $+300$ , and (10)  $+350$  mV vs NHE.

accumulation time was 15 and 150 s, respectively. Taking these data into account, the enhancement factor was calculated to be  $10^5$ . The SERRS intensity increased by a factor of up to 4 on the newly developed surface compared to previous experiments with cytochrome *c* adsorbed on electrochemically roughened silver electrodes. The enhancement factor for electrochemically modified silver substrates is known to be in the range of  $2 \times$

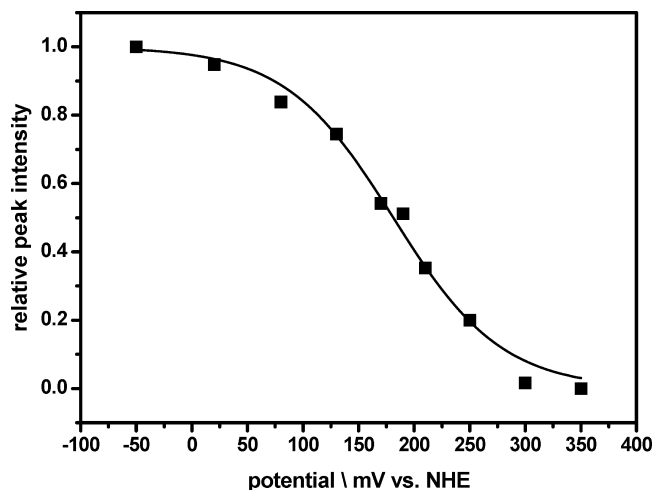


**Figure 11.** Relative intensity of the  $\nu_4$  band at  $1361 \text{ cm}^{-1}$  plotted vs the applied potential. Solid squares represent the experimental data. The solid line is the fit eq 2 providing a calculated standard potential of  $E_m = 181 \text{ mV}$ .

$10^4$ ,<sup>21</sup> which is in line with the calculated EF of  $10^5$  for the novel silver substrate modified with AgNPs.

In order to test the electrochemical activity of the newly developed SER(R)S-active silver substrate, a spectroelectrochemical titration of cc was performed. Cytochrome *c* was adsorbed on a SAM of ME. Changing the applied potential stepwise between  $-50$  and  $+350$  mV vs NHE, SERR spectra were taken (Figure 10). The protein showed a transition from the reduced to the oxidized state, as deduced from the  $\nu_4$  band changing from  $1361$  to  $1374 \text{ cm}^{-1}$ . This corresponds to our previous studies on cc on electrochemically roughened silver electrodes.<sup>18</sup> The relative intensity of the  $\nu_4$  band at  $1361 \text{ cm}^{-1}$  was plotted as a function of applied potential (Figure 11) and fitted to the sigmoidic function



$$I_{\text{SERRS}} = \frac{1}{1 + \exp[(E - E_{\text{ip}})/\varphi]} \quad (2)$$

where  $I_{\text{SERRS}}$  denotes the relative intensity of the  $\nu_4$  band at  $1361 \text{ cm}^{-1}$ .  $E_{\text{ip}}$  is the potential of the inflection point, which reflects the midpoint potential  $E_{\text{m}}$  of the redox center, and  $\varphi$  is a scaling factor. Ideally,  $\varphi = RT/F \approx 26 \text{ mV}$ , and  $E_{\text{ip}} = E_{\text{m}}$  in accordance with the Nernst equation.  $E_{\text{ip}}$  revealed a midpoint potential of  $E_{\text{m}} = 181 \pm 4 \text{ mV}$ , and the scaling factor was  $\varphi = 49 \text{ mV}$ . From this we can conclude that cc adsorbed to a monolayer of ME can be electrochemically reduced and oxidized on the newly developed SERR-active surface.

## Conclusion

In this study we developed a SERRS-active surface by assembling a monolayer of Ag NPs on a silver plane. Varying the number of NPs per unit area the enhancement factor could be tuned so as to exceed that of electrochemically roughened silver electrodes. Under optimum conditions the total average enhancement factor calculates to  $10^5$ . The enhancement factor was shown to be determined largely by the number of explicitly isolated NPs rather than NP clusters. This effect could be explained in terms of LSPs equivalent to NPs on nonconducting surfaces such as glass. Distances between single NPs were not small enough to play a decisive role for the enhancement factor at the particular wavelength used (413 nm). The conducting underlayer of the Ag plane, on the other hand, does not seem to be prohibitive for the surface enhancement, while it allowed the application of spectroelectrochemistry. This was tested by potentiostatic titration of cc adsorbed on a SAM of ME. The results demonstrate an electrochemical activity similar to electrochemically roughened electrodes.

In the context of spectroelectrochemistry, the newly developed surface has the potential to replace electrochemically roughened silver as a standard substrate for SER(R)S measurements.

## References and Notes

- (1) Kneipp, K.; Kneipp, H.; Itzkan, I.; Dasari, R. R.; Feld, M. S. *J. Phys.: Condens. Matter* **2002**, *14*, R597.

- (2) Ryder, A. G. *Curr. Opin. Chem. Biol.* **2005**, *9*, 489.
- (3) Maquelin, K.; Kirschner, C.; Choo-Smith, L. P.; van den Braak, N.; Endtz, H. P.; Naumann, D.; Puppels, G. J. *J. Microbiol. Methods* **2002**, *51*, PII S0167.
- (4) Hanlon, E. B.; Manoharan, R.; Koo, T. W.; Shafer, K. E.; Motz, J. T.; Fitzmaurice, M.; Kramer, J. R.; Itzkan, I.; Dasari, R. R.; Feld, M. S. *Phys. Med. Biol.* **2000**, *45*, R1.
- (5) Edwards, H. G. M.; Newton, E. M.; Dickensheets, D. L.; Wynn-Williams, D. D. *Spectrochim. Acta, Part A* **2003**, *59*, 2277.
- (6) Fleischmann, M.; Hendra, P. J.; McQuillan, A. J. *Chem. Phys. Lett.* **1974**, *26*, 163.
- (7) Jeanmaire, D. L.; Van Duyne, R. P. *J. Electroanal. Chem.* **1977**, *84*, 1.
- (8) Albrecht, M. G.; Creighton, J. A. *J. Am. Chem. Soc.* **1977**, *99*, 5215.
- (9) Moskovits, M. *Rev. Mod. Phys.* **1985**, *57*, 783.
- (10) Devoe, H. J. *Chem. Phys.* **1964**, *41*, 393.
- (11) Devoe, H. J. *Chem. Phys.* **1965**, *43*, 3199.
- (12) Gunnarsson, L.; Rindzevicius, T.; Prikulis, J.; Kasemo, B.; Kall, M.; Zou, S. L.; Schatz, G. C. *J. Phys. Chem. B* **2005**, *109*, 1079.
- (13) Tamaru, H.; Kuwata, H.; Miyazaki, H. T.; Miyano, K. *Appl. Phys. Lett.* **2002**, *80*, 1826.
- (14) Svedberg, F.; Li, Z. P.; Xu, H. X.; Kall, M. *Nano Lett.* **2006**, *6*, 2639.
- (15) Romero, I.; Aizpurua, J.; Bryant, G. W.; de Abajo, F. J. G. *Opt. Express* **2006**, *14*, 9988.
- (16) Lombardi, J. R.; Birke, R. L. *J. Phys. Chem. C* **2008**, *112*, 5605.
- (17) Lombardi, J. R.; Birke, R. L.; Lu, T. H.; Xu, J. J. *Chem. Phys.* **1986**, *84*, 4174.
- (18) Grosserueschkamp, M.; Friedrich, M. G.; Plum, M.; Knoll, W.; Naumann, R. L. C. *J. Phys. Chem. B* **2009**, *113*, 2492.
- (19) Kranich, A.; Ly, H. K.; Hildebrandt, P.; Murgida, D. H. *J. Am. Chem. Soc.* **2008**, *130*, 9844.
- (20) Murgida, D. H.; Hildebrandt, P.; Wei, J.; He, Y. F.; Liu, H. Y.; Waldeck, D. H. *J. Phys. Chem. B* **2004**, *108*, 2261.
- (21) Taylor, C. E.; Pemberton, J. E.; Goodman, G. G.; Schoenfish, M. H. *Appl. Spectrosc.* **1999**, *53*, 1212.
- (22) Wen, R.; Fang, Y. J. *Colloid Interface Sci.* **2005**, *292*, 469.
- (23) Atay, T.; Song, J. H.; Nurmikko, A. V. *Nano Lett.* **2004**, *4*, 1627.
- (24) Enustun, B. V.; Turkevich, J. *J. Am. Chem. Soc.* **1963**, *85*, 3317.
- (25) Frens, G. *Kolloid Z. Z. Polym.* **1972**, *250*, 736.
- (26) Hu, S. Z.; Morris, I. K.; Singh, J. P.; Smith, K. M.; Spiro, T. G. *J. Am. Chem. Soc.* **1993**, *115*, 12446.
- (27) Ru, E. C. L.; Blackie, E.; Meyer, M.; Etchegoin, P. G. *J. Phys. Chem. C* **2007**, *111*, 13794.
- (28) Haas, A. S.; Pilloud, D. L.; Reddy, K. S.; Babcock, G. T.; Moser, C. C.; Blasie, J. K.; Dutton, P. L. *J. Phys. Chem. B* **2001**, *105*, 11351.

JP905598G